A first principles study of CH 3 dehydrogenation on Ni(111)

A. Michaelides and P. Hu

Citation: The Journal of Chemical Physics **112**, 8120 (2000); doi: 10.1063/1.481412
View online: http://dx.doi.org/10.1063/1.481412
View Table of Contents: http://scitation.aip.org/content/aip/journal/jcp/112/18?ver=pdfcov
Published by the AIP Publishing

A first principles study of CH_3 dehydrogenation on Ni(111)

A. Michaelides and P. Hu[a)]
School of Chemistry, The Queen's University of Belfast, Belfast BT9 5AG, United Kingdom

(Received 12 January 2000; accepted 16 February 2000)

Density functional theory with gradient corrections and spin polarization has been used to study the dehydrogenation of CH_3 on Ni(111), a crucial step in many important catalytic reactions. The reaction, $CH_{3(ads)} \rightarrow CH_{2(ads)} + H_{(ads)}$, is about 0.5 eV endothermic with an activation energy of more than 1 eV. The overall reaction pathway is rather intriguing. The C moiety translates from a hcp to a fcc site during the course of the reaction. The transition state of the reaction has been identified. The CH_3 species is highly distorted, and both C and the active H are centered nearly on top of a row of Ni atoms with a long C–H bond length of 1.80 Å. The local density of states coupled with examination of the real space distribution of individual quantum states has been used to analyze the reaction pathway. © *2000 American Institute of Physics.* [S0021-9606(00)30218-5]

I. INTRODUCTION

Small hydrocarbon species, such as methyl fragments, have been implicated as intermediates in a variety of industrial catalytic processes. A detailed knowledge of the surface chemistry of these hydrocarbon species on metal surfaces will therefore be invaluable to our understanding of the corresponding catalytic processes. Consequently, methyl groups have been extensively studied both experimentally and theoretically on a variety of catalytic surfaces.[1–11] The dehydrogenation of CH_3 is an important elementary step in fundamental catalytic processes such as steam reforming and methanation. It is also an archetypal α-H elimination process. In the present study, we have determined the microscopic reaction pathway and activation energy for the dehydrogenation of methyl to methylene on Ni(111). In addition we have also attempted to identify the underlying chemical principles that control this particular reaction process.

Methyl groups tends to be rather unstable on most transition metal surfaces. As a consequence of this instability direct experimental data about the chemistry of these species is difficult to obtain. Zaera and co-workers[12–14] as well as Bent and co-workers[15,16] have generated CH_3 groups on various transition metals from adsorbed methyl halides and have examined the balance between oxidative addition, reductive elimination and C–C coupling. Tjandra and Zaera[14] have concluded, for Ni(111), that in the low coverage regime CH_3 groups tend to dehydrogenate into adsorbed C and H. As the coverage increases, hydrogenation to methane becomes the dominant process. Clearly there is a delicate balance determining whether methyl gains or loses hydrogen.

Theoretical methods have been extensively employed in the study of CH_3 fragments adsorbed on transition metal surfaces, providing important data concerning the thermodynamics of CH_x interconversion. Yang and Whitten[7,17–20] have performed *ab initio* embedded cluster calculations to model CH_x fragments on Ni(111). They calculated adsorption energies, Ni–C bond lengths, and C–H stretching frequencies and have found that all CH_x fragments bind strongly at threefold and bridge sites. Yang and Whiten have also studied some $CH_x + H$ association reactions, including $CH_2 + H \rightarrow CH_3$.[7] Siegbahn and Panas[21] have carried out bond prepared cluster calculations to model CH_x groups chemisorbed on Ni(100) and Ni(111). Calculated adsorption energies and optimized structures were reported. Van Santen and co-workers[22–26] have carried out density functional cluster calculations on methane activation and dehydrogenation in which the specific adsorption sites of CH_x fragments were discussed. Recently, Kua and Goddard[8] as well as Paul and Sautet,[9] both using density functional methods, have studied CH_x chemisorption on Pt(111) and Pd(111), respectively.

Here we present the first DFT calculations for the methyl dissociation reaction on Ni(111), going from adsorbed methyl to adsorbed methylene and hydrogen. The paper is organized as follows. Below, some of the details of our total energy calculations are outlined. We report and discuss our results in Sec. III. In the first part of Sec. III, the total energy change for the CH_3 dissociation reaction is discussed. In the second and third parts the reaction pathway is detailed and discussed. The conclusions are outlined in the final section.

II. CALCULATIONS

Ab initio total energy calculations within the DFT framework[27–29] were carried out in this study. The basis set consists of plane waves. A Fermi smearing of 0.1 eV was utilized and the corrected energy extrapolated to zero temperature, which considerably reduces **k**-point sampling. All calculations were spin polarized. The generalized gradient approximation of Perdew and Wang[30] was utilized throughout.

Ab initio nonlocal pseudopotentials[31] of C, H, and Ni in fully separable Kleinman–Blylander form[32] up to a 550 eV cutoff were used. The supercell approach was employed to model periodic geometries. The Ni(111) surface was represented by a three layer Ni slab with a large vacuum region between slabs. Because the calculations were carried out us-

a)Author to whom correspondence should be addressed. Fax: (+44) 1232 382117; electronic mail: p.hu@qub.ac.uk

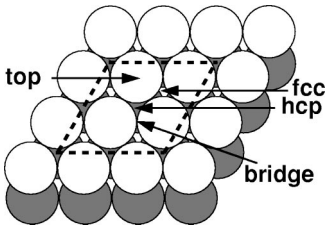

FIG. 1. Top view of the Ni(111) surface. The dashed lines represent the surface unit cell, the arrows indicate the position of the four high symmetry sites. For clarity, only two Ni layers are shown.

ing spin polarization, with the corresponding increase in computational load, we fixed the Ni atoms at bulk truncated positions. A $p(2\times2)$ unit cell was used (Fig. 1) and the adsorbates were placed on one of the two surfaces. A Monkhorst–Pack mesh[33] with a $2\times2\times1$ **k**-grid sampling, in the surface Brillouin zone, was found to offer sufficient accuracy. This is an identical chemisorption model to that used in previous studies[10,34] and tests concerning the accuracy of this model and the isolated systems have been reported therein.

We searched for low energy pathways taking us from CH_3–Ni(111) to CH_2/H–Ni(111) using a constrained minimization technique.[35] In this approach we keep the C–H distance fixed at preselected values and minimize the total energy with respect to all remaining degrees of freedom. In particular this means that the molecules are free to rotate and translate subject to the above constraint. The transition state is identified when (i) the energy along the reaction coordinate is a maximum, but a minimum with respect to all remaining degrees of freedom, and (ii) the forces on the atoms vanish.[36]

III. RESULTS AND DISCUSSION

A. CH_3 dissociation

We first consider the chemisorption of the atomic and molecular fragments involved. The Ni(111) surface exhibits four high symmetry adsorption sites; top, bridge, and two threefold hollow sites, shown in Fig. 1. The threefold hollow sites differ only in their relationship with the second layer: The hcp threefold hollow site has a Ni atom directly below it, while the fcc threefold hollow site has a Ni atom only in the third layer. The calculated chemisorption energies of CH_3, CH_2, and H are detailed in Table I. The threefold hollow sites are the preferred sites for all adsorbates. CH_3 marginally favors the hcp hollow site over the fcc hollow site with a chemisorption energy of 1.48 eV,[10] CH_2 and H both prefer fcc hollow sites, binding more strongly than CH_3, with chemisorption energies of 3.26 eV and 2.60 eV,[34] respectively. Good agreement between these values and recent experimental and theoretical results is found where direct comparison is available.

TABLE I. Chemisorption energies in eV for CH_3, CH_2, and H on the high symmetry sites of Ni(111).

	hcp	fcc	bridge	top
CH_3	1.48	1.46	1.37	1.22
CH_2	3.22	3.26	3.14	2.36
H	2.54	2.60	…	…

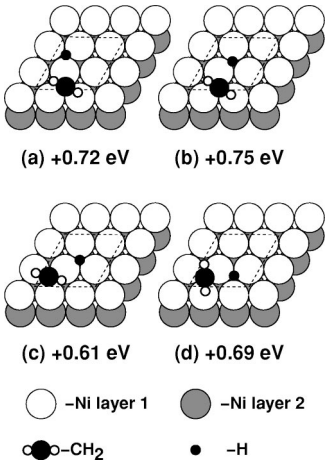

FIG. 2. The four CH_2/H coadsorption arrangements identified within the $p(2\times2)$ unit cell. The energies of these arrangements relative to CH_3 chemisorbed on an hcp site are also shown. The periodic nature of the systems are not shown for clarity.

The enthalpy change (ΔH) of the reaction $CH_{3(ads)}\rightarrow CH_{2(ads)}+H_{(ads)}$ has been determined by two alternative methods. The first was by comparing the total energy of chemisorbed methyl (CH_3–Ni(111)) with the total energy of coadsorbed methylene and hydrogen (CH_2/H–Ni(111)),

$$\Delta H = E_{CH_2H/Ni(111)} - E_{CH_3/Ni(111)},$$

where $E_{CH_2/H/Ni(111)}$ and $E_{CH_3/Ni(111)}$ are the total energies of Ni(111)-$p(2\times2)$-(CH_2–H) and Ni(111)-$p(2\times2)$-CH_3, respectively. Several stable coadsorption arrangements of CH_2 and H, all of which have a similar energy, have been identified. These are shown in Fig. 2. The energies of these states relative to CH_3 chemisorbed at a hcp site are also shown. The most stable coadsorption arrangement identified, Fig. 2(c), has CH_2 and H coadsorbed close to fcc and hcp sites, respectively. The reaction, $CH_{3(ads)}\rightarrow CH_{2(ads)}+H_{(ads)}$ going from CH_3 initially adsorbed at a hcp site to coadsorption arrangement (c), is therefore 0.61 eV endothermic. Because of the small energetic differences between the four coadsorption arrangements it is conceivable that any one of these could be the final state, within the unit cell, of the dissociation reaction.

The second method by which the enthalpy change of the reaction has been determined was by combining the energies of a separate chemisorbed hydrogen and a separate chemisorbed methylene and comparing them to a chemisorbed methyl,

$$\Delta H = [E_{CH_2/Ni(111)} + E_{H/Ni(111)} - E_{Ni(111)}] - E_{CH_3/Ni(111)},$$

where $E_{CH_2/Ni(111)}$, $E_{H/Ni(111)}$, $E_{Ni(111)}$, and $E_{CH_3/Ni(111)}$ are the total energies of Ni(111)-$p(2\times2)$-CH_2, Ni(111)-$p(2\times2)$-H, Ni(111)-$p(2\times2)$, and Ni(111)-$p(2\times2)$-CH_3, respectively. By this method the reaction is determined to be endothermic by 0.51 eV. This total energy change differs by about 0.1 eV from the previous one. The principal reason for

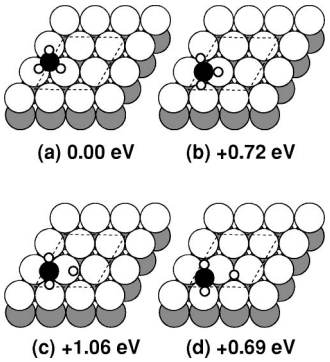

FIG. 3. The lowest energy reaction pathway identified for CH_3 dehydrogenation on Ni(111). (c) is the transition state. For clarity, the periodic nature of the systems is not shown.

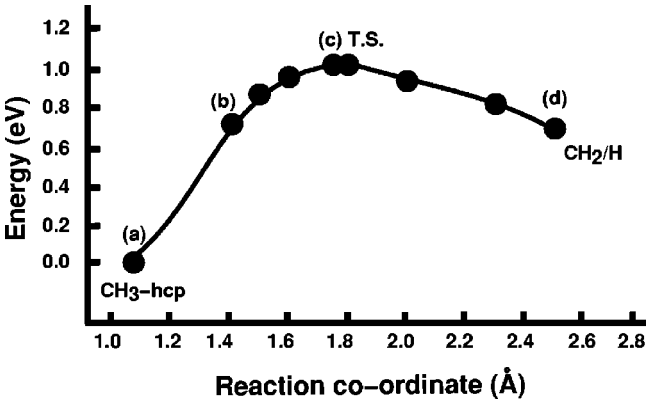

FIG. 4. Total energy in eV, relative to the initial state, for the lowest energy reaction pathway. The reaction coordinate in Å is the distance between carbon and the active hydrogen. (a), (b), (c), and (d) refer to the points shown in Fig. 3. The solid line is an aid to the eye.

this is that when CH_2 and H are coadsorbed within the same $p(2\times2)$ unit cell they are still close enough to compete for bonding with the same Ni atoms.[37,38]

The enthalpy change for this reaction has not been determined experimentally, and thus it is with theory alone that we make comparison. Very good agreement is found with the embedded cluster CI calculations of Yang and Whitten.[7] They calculated the reaction to be 0.57 eV endothermic. Reasonable agreement is also found with the DFT cluster calculations of van Santen and co-workers.[25] They quoted an energy range of between 0.26 and 0.42 eV. Siegbahn and Panas,[21] using a bond prepared cluster approach, obtained a value of 0.35 eV. Using the empirical bond order conservation Morse potential method Bell and Schustorovich[39] determined a value of 0.52 eV.

Spin restricted calculations have also been performed, yielding an enthalpy change for the reaction of only $+0.2$ eV. The reason for the large discrepancy between the spin polarized and the spin restricted calculations is that the adsorbates, particularly CH_2 in the final state, bind more strongly to the surface when spin polarization effects are neglected.[10] Clearly spin restricted calculations are inadequate for this reaction.

B. Dissociation pathway

Figures 3 and 4 show snapshots and the energy profile of the lowest energy reaction pathway identified. Table II lists some important geometrical parameters along this pathway. The pathway consists of the following sequence of events. Initially CH_3 is adsorbed at a hcp hollow site with its C–H bonds aligned to the underlying Ni atoms [Fig. 3(a)]. As one of the C–H bonds is stretched, CH_3 starts to translate towards a bridge site. The other two hydrogens of CH_3 begin to move into a plane with the carbon normal to the surface [Fig. 3(b)]. The C–Ni distance shortens indicative of greater CH_2 character. At the transition state [Fig. 3(c)] the methyl fragment is highly distorted. The active C–H bond is stretched to 1.80 Å. The C–Ni bond length has decreased from 2.28 Å to 1.95 Å. Such a value is closer to that found in chemisorbed CH_2 (1.97 Å). The transition state structure more closely resembles the products than the reactant. Carbon and the active H rest nearly along a row of Ni atoms, displaced from the center of the Ni row by about 0.2 towards fcc hollow sites. The C of the reaction complex is in fact very close to a bridge site. Following the transition state both CH_2 and H fall from the row of Ni atoms towards fcc hollow sites, i.e., coadsorption arrangement (d) [Fig. 3(d)]. This is a very unusual reaction pathway. The C moiety has in fact translated across a bridge site during the course of the reaction going from a hcp to a fcc threefold hollow site. This considerable movement of the C moiety is surprising for such a simple chemical process as dehydrogenation.

The orientation of the pseudo methyl about the transition state has been further examined. If the center of mass of the reaction complex is fixed along the center of the Ni atom row then the energy increases by only 0.03 eV compared to the true transition state. If the reaction complex is displaced to the hcp side of the Ni–Ni bridge an alternative transition state, only 0.04 eV less stable, has been detected. Clearly the potential energy surface is quite flat in this region. Therefore, it should be stressed that CH_2 and H need not necessarily fall into coadsorption arrangement (d) as they also have the possibility of falling into any of the other three coadsorption arrangements (Fig. 2).

Reaction pathways have also been studied with CH_3 initially placed at each of the other high symmetry sites (fcc, bridge, top) of Ni(111). It was found that an equivalent transition state, the same as that reported previously [Fig. 3(c)], was accessed from all sites. The pathway determined when CH_3 is initially placed on an fcc site is worth mentioning since CH_3 chemisorption is only 0.02 eV less stable at this site compared to the hcp site. As one of the C–H bonds is stretched CH_3 translates towards a bridge site and accesses an identical transition state to that discussed above [Fig. 3(c)]. After the transition state the pathway is the same as that discussed above with CH_2 and H falling into neighboring fcc sites, i.e., coadsorption arrangement (d). In this pathway the C moiety, therefore, also makes an unusual movement translating from an fcc threefold hollow site towards a bridge site and then back again to the same fcc site.

The activation energy for the lowest energy reaction pathway identified is 1.06 eV (Fig. 4). This value is in agreement with that determined by Bell and Schustorovich.[39] Us-

TABLE II. Structural parameters at selected points along the reaction pathway. C-surf and H-surf are the C and H-surface perpendicular distances, respectively. α is the surface-C–H angle, where H is the active H that is removed from CH_3.

	(a) CH_3 hcp	(b) C–H:1.40 Å	C–H:1.60 Å	(c) C–H:1.80 Å	(d) CH_2/H	CH_2-fcc	H-fcc
C–Ni (Å)	2.28	2.07	1.99	1.95	1.97	1.97	···
C-surf (Å)	1.76	1.70	1.61	1.55	1.42	1.44	···
H–Ni (Å)	2.21	1.77	1.60	1.55	1.69	1.75	1.75
H-surf (Å)	2.18	1.76	1.53	1.40	0.98	0.98	0.99
α (°)	111.81	92.42	87.46	85.25	···	···	···

ing the bond order conservation Morse potential method they calculated a zero coverage activation energy of 1.04 eV. Yang and Whitten[7] have also examined this reaction, determining both an activation energy and a reaction pathway. To the best of our knowledge, this is the only time prior to ours that an attempt to determine the microscopic reaction pathway on Ni(111) has been made. They considered the reverse process, $CH_{2(ads)}+H_{(ads)}\rightarrow CH_{3(ads)}$. The reaction pathway, which they identified, is different from ours. They suggested that the CH_3 group should first rotate in a threefold hollow site (hcp) by 60°. The C–H bonds of CH_3 would then be directed towards Ni–Ni bridge sites. A C–H bond would then break across one of these bridge sites. They determined a barrier for this process of over 2 eV. We investigated their pathway by rotating CH_3 in both the hcp and fcc threefold hollow sites. The energy of the system rises by about 0.2 eV upon rotation.[10] One of the C–H bonds was then stretched. At both sites the pseudo CH_3 group rotated so that the active H could get closer to one of the Ni atoms of the Ni–Ni bridge. Simultaneously the CH_3 fragment migrated towards the bridge site until the same transition state as that reported earlier was accessed [Fig. 3(c)]. A pathway of the type described by Yang and Whitten could not be identified. A possible explanation for this is that in the calculations of Yang and Whitten a larger number of atomic degrees of freedom were held fixed. The C of CH_3 was fixed above the hcp hollow site and the geometries of the highest energy point were not optimized. In fact Yang and Whitten remarked that the barrier that they had identified was a factor of 2 higher than the barrier which they had determined for the $CH+H\rightarrow CH_2$ association reaction. They suggested that a pathway with a lower activation energy may exist.

Studies carried out by Tiandra and Zaera[14] on the thermal stabilities of methyl iodide on Ni(111) indicate that surface CH_3 undergoes either hydrogenation to form gas phase CH_4 or dehydrogenation to form surface carbon. The partitioning of methyl between these two reaction routes depends upon the surface coverage of CH_3 and H. At CH_3 coverages >0.17 ML hydrogenation of CH_3 to CH_4 becomes the more facile reaction channel. In the present study the CH_3 surface coverage is 0.25 ML, therefore, it is expected that the barrier for CH_3 dehydrogenation to CH_2 and H is higher than the barrier for CH_3 hydrogenation to CH_4. In a previous study[11] with a system identical to the present one, the activation energy for the hydrogenation reaction was determined to be 0.85 eV. It is clear that the dehydrogenation reaction barrier ($E_{act}=1.06$ eV) is higher than that of the hydrogenation reaction ($E_{act}=0.85$ eV) which is consistent with the experimental work of Tjandra and Zaera.[14] This comparison is not ideal though, because in the experiments of Tjandra and Zaera coadsorbed iodine was present.

The reaction pathway that we have identified can provide some insight into the partial oxidation of methane into methanol. A key to realize this reaction on a metal surface is to stabilize chemisorbed CH_3. A problem with most transition metal catalysts is that if they are capable of activating methane, then they also readily break the remaining C–H bonds of CH_3. It is expected that if an isolated metal atom were used as a catalytic center then the reaction barrier for CH_3 dehydrogenation would be greater while the reaction barrier for methane dissociation may not change as much since the transition state for the latter reaction is located above a single metal atom.[11] In fact, this is consistent with a recent experimental work which showed that methane could be readily converted into a methane derivative using a catalyst containing single Pt atoms, while the C yield increased (indicative of further dehydrogenation) if the Pt atoms were reduced to Pt clusters.[40]

C. Analysis

The reaction pathway has been analyzed with the local density of states (LDOS) coupled with examination of the real space distribution of individual quantum states. Figure 5 shows LDOS plots for CH_2, CH_3, and H on Ni(111). In two previous papers we analyzed the bonding of these adsorbates to Ni(111) in some detail.[10,34] Here we will briefly discuss the essential bonding characteristics of each system. Following this we will consider the orbital changes that occur upon going from reactant to product.

Figure 5(b) illustrates the LDOS projected onto C of CH_3 when CH_3 is adsorbed at the hcp threefold hollow site. The first peak in Fig. 5(b) (going from low to high energies) at 13 eV below the Fermi level (E_f) is composed of states which are predominantly of molecular character, $2a_1$ bonding states of CH_3. The $2a_1$ orbital in gas phase CH_3 is the lowest energy orbital of CH_3, a combination of a C $2s$ and three H $1s$ orbitals. States within the second peak (about 6 eV below E_f) are of e_1 character mixed with Ni d. In gas phase CH_3 the e_1 orbitals are a degenerate pair of C–H bonding orbitals. They are the principal C–H bonding orbitals of CH_3, each being composed of a C p and H s orbitals. When CH_3 chemisorbs on Ni(111) the e_1 orbitals of CH_3 mix with Ni d states, resulting in a three-center interaction

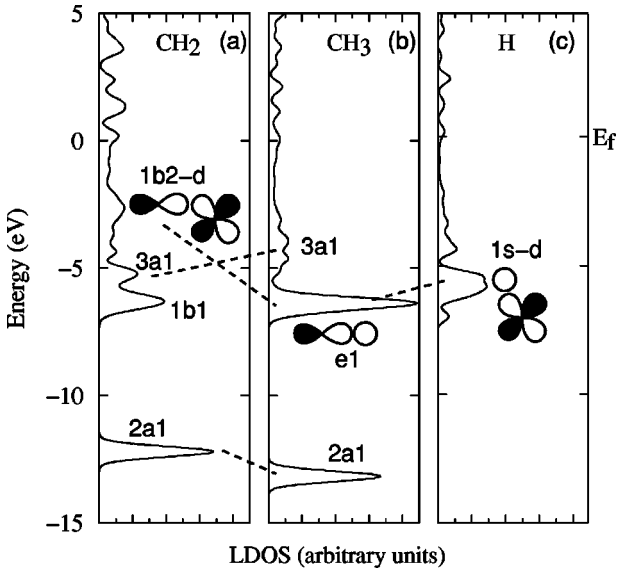

FIG. 5. Local densities of states plots (LDOS) for CH_2, CH_3, and H at their preferred chemisorption sites on Ni(111). The Fermi levels (E_f) of each system have been aligned to 0 eV. A partial energy level interaction diagram has been superimposed upon the plots highlighting the most significant orbital changes that occur upon going from $CH_{3(ads)}$ to $CH_{2(ads)}+H_{(ads)}$.

between C, H, and Ni;[10] as shown in Fig. 6(a). Following the second peak there is a broad energy continuum up to the Fermi level. At the lower end of this continuum (about 4 eV below E_f) several small peaks are just about discernible and states of $3a_1$ character can be seen within these peaks. In gas phase CH_3 the $3a_1$ orbital is the highest energy molecular orbital and is singly occupied. Upon adsorption it projects directly into the surface, forming bonds of σ character with the surface.

Figure 5(a) illustrates the LDOS projected onto C of CH_2 when CH_2 is adsorbed at the fcc threefold hollow site. The first peak in Fig. 5(a) at 12 eV below E_f is composed of states that are predominantly $2a_1$ bonding states of CH_2. The $2a_1$ orbital in gas phase CH_2 is the lowest energy orbital of CH_2, a combination of a C $2s$ and two H $1s$ orbitals. The $2a_1$ derived peak of CH_2 in Fig. 5(a) is about 1 eV higher in energy than that of CH_3 in Fig. 5(b). This is because the $2a_1$ orbital of CH_2 is less delocalized than that of CH_3 since it is derived from only two H $1s$ orbitals compared to the CH_3-$2a_1$ orbital which is derived from three H $1s$ orbitals. States within the second peak (7 eV below E_f) are of $1b_1$ character mixed slightly with Ni d. In gas phase CH_2 the $1b_1$ orbital is a C–H bonding orbital analogous to the e_1 orbitals of CH_3. Since there is only a single $1b_1$ orbital in gas phase CH_2 (compared to the pair of e_1 orbitals in CH_3) this peak is about half as large as the e_1 derived peak in the CH_3 chemisorption system [Fig. 5(b)]. The third peak in Fig. 5(a) (about 5 eV below E_f) represents $3a_1$ states of CH_2 mixed with Ni d. The $3a_1$ orbital of CH_2, as in CH_3, projects directly into the surface. These states reside at slightly lower energies and are more localized around C in CH_2 than in CH_3. Within the small peak at 3 eV below E_f are states of $1b_2$ character. The $1b_2$ orbital of CH_2 is essentially a C p orbital. When CH_2 is chemisorbed this orbital lies parallel to and forms bonds of π character with the surface.

Figure 5(c) illustrates the LDOS projected onto H chemisorbed at the fcc threefold hollow site. One clear peak at about 6 eV below E_f is observed. States within this peak are principally H s Ni d bonding states.

Upon the transformation of $CH_{3(ads)}$ to $CH_{2(ads)}$ and H(ads) the chemical changes are (i) a C–H bond breaks; (ii) a H-surface bond is created; and (iii) an alkyl surface bond is converted into an alkylidene surface bond. These changes are clearly seen in the LDOS plots of Fig. 5 upon which an energy level interaction diagram has been superimposed. The interaction diagram in Fig. 5 highlights the fact that the transformation of $CH_{3(ads)}$ to $CH_{2(ads)}$ and $H_{(ads)}$ is intimately associated with the e_1 derived states of CH_3. As the C–H bond breaks certain e_1 orbitals (corresponding to the C–H bond that is being broken) split into H $1s$ and C p orbitals. As outlined above the $1s$ orbital of the chemisorbed H contributes to the H-surface bond [Fig. 5(c)]. The C p orbital derived from the ruptured e_1 orbital of CH_3 is in fact the $1b_2$ orbital of CH_2. As mentioned above, orbitals of this type lie parallel to and mix with surface Ni atoms. It is this extra bonding of CH_2 with the surface that transforms that alkyl surface bond into an alkylidene surface bond.

The catalytic role of the substrate is nicely illustrated in Fig. 5. The gas phase dissociation of $CH_{3(gas)}$ to $CH_{2(gas)}$ and $H_{(gas)}$ is endothermic by about 5 eV [experiment 4.8 eV (Ref. 41), 5.0 eV from our calculations]. On the Ni surface, however, the reaction is endothermic by only about 0.5 eV. The reason for this, as we have just seen, is that on the surface the $1b_2$ and H $1s$ orbitals that are formed upon cleavage of the C–H bond are stabilized by mixing with Ni states. In the gas phase no such stabilization is possible and the $1b_2$ and H $1s$ orbitals remain at high energies.

Coupled with decreasing the overall exothermicity of the

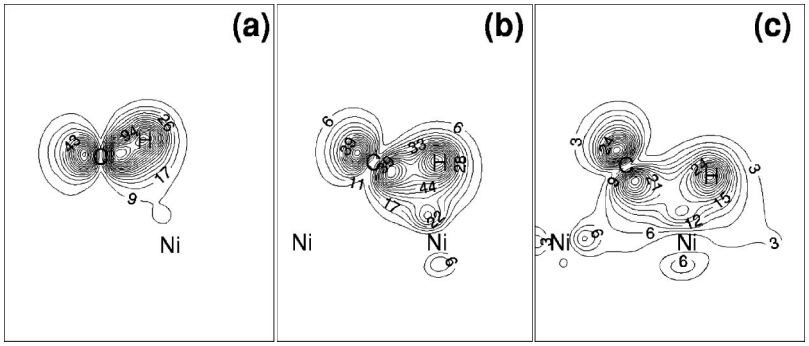

FIG. 6. 2D electron density contour plots for an e_1 derived quantum state at certain points along the reaction pathway. The quantum states in (a), (b), and (c) are taken from the points (a), (b), and (c), in Fig. 3. The planes of the 2D cuts are through the C–H bond normal to the surface. Density is plotted in units of 3.63×10^{-3} electrons/bohr^3.

TABLE III. Total number of valence electrons within certain radii centered on the nuclei of C and the active H at various points along the reaction pathway. (a), (b), (c), and (d) refer to (a), (b), (c), and (d) of Fig. 3.

	(a) CH_3-hcp	(b) C–H:1.40 Å	C–H:1.60 Å	(c) C–H:1.80 Å	(d) CH_2/H	CH_2-fcc	H-fcc
C(0.5 Å)	0.845	0.811	0.808	0.807	0.817	0.816	⋯
C (0.8 Å)	2.610	2.506	2.484	2.484	2.510	2.505	⋯
H(0.5 Å)	0.456	0.363	0.345	0.345	0.373	⋯	0.373

reaction, the Ni surface also stabilizes the C–H bond as it is stretched. In the gas phase, the energy cost of the bond stretch is mostly felt by an e_1 molecular orbital. The energy of this orbital rises dramatically and continuously upon dissociation. On the surface, although certain e_1 derived states are also destabilized, their energy and consequently the total energy of the system does not rise as dramatically as in the gas phase. This is because the e_1 derived states are stabilized by mixing with Ni d states. Figure 6 shows a typical e_1 derived state at certain points along the reaction pathway. Initially [Fig. 6(a)] the e_1 derived state mixes slightly with d orbitals of a surface Ni. As the C–H bond is stretched [Fig. 6(b)] the e_1 derived state mixes more strongly with the Ni. At the transition state [Fig. 6(c)] the electrons within this quantum state are delocalized about the three atoms. This allows the quantum state to lower its eigenvalue compared to the gas-phase reaction. After the transition state the electrons become less delocalized, redistributing around the C and H nuclei again.

Finally, charge delocalization is a general feature of this transition state. This is illustrated in Table III, which shows the total number of valence electrons around C and H at various stages throughout the reaction. The density around C and H reaches a minimum at the transition state indicating that charge is delocalized with less located close to C and H.

IV. CONCLUSIONS

Density functional theory with gradient corrections and spin polarization has been used to study the dehydrogenation of CH_3 on Ni(111). The reaction, $CH_{3(ads)} \rightarrow CH_{2(ads)} + H_{(ads)}$, is found to be about 0.5 eV endothermic, and is a highly activated process with an activation energy in excess of 1 eV. The transition state has been identified, and the CH_3 species in the transition state is very distorted and has moved from its favored chemisorption site. At the transition state the activated methyl is centered nearly on top of a row of Ni atoms and a long C–H bond length of 1.80 Å is observed. The metal substrate plays an important role in stabilizing very particular C–H bonding orbitals during the course of the reaction.

ACKNOWLEDGMENTS

Sincere thanks to The Supercomputing Center for Ireland for computer time. A.M. wishes to thank EPSRC for a studentship.

[1] F. Zaera, Chem. Rev. **95**, 2651 (1995).
[2] B. E. Bent, Chem. Rev. **96**, 1361 (1996).
[3] L.-X. Zhou and J. M. White, Surf. Sci. **241**, 270 (1991).
[4] J. C. Wenger, D. J. Oakes, M. R. S. Mc. Coustra, and M. A. Chesters, Surf. Sci. **360**, 81 (1996).
[5] D. Howard Fairbrother, X. D. Peng, R. Viswanathan, P. C. Stair, M. Trenary, and J. Fan, Surf. Sci. Lett. **285**, L455 (1993).
[6] Q. Y. Yang, K. J. Maynard, A. D. Johnson, and S. T. Ceyer, J. Chem. Phys. **102**, 7734 (1995).
[7] H. Yang and J. L. Whitten, J. Am. Chem. Soc. **113**, 6442 (1991).
[8] J. Kua and W. A. Goddard, J. Phys. Chem. B **102**, 9481 (1999); **102**, 9492 (1999).
[9] J.-F. Paul and P. Sautet, J. Phys. Chem. B **102**, 1578 (1998).
[10] A. Michaelides and P. Hu, Surf. Sci. **437**, 362 (1999).
[11] A. Michaelides, P. Hu, and A. Alavi, J. Chem. Phys. **111**, 1343 (1999).
[12] F. Zaera and H. Hoffmann, J. Phys. Chem. **95**, 6297 (1991).
[13] F. Zaera, Catal. Lett. **11**, 95 (1991).
[14] S. Tjandra and F. Zaera, J. Catal. **147**, 598 (1994).
[15] C.-M. Chiang, T. H. Wentzlaff, and B. E. Bent, J. Phys. Chem. **96**, 1836 (1992).
[16] J.-L. Lin and B. E. Bent, Chem. Phys. Lett. **194**, 208 (1992).
[17] J. L. Whitten and H. Yang, Surf. Sci. Rep. **218**, 55 (1996).
[18] H. Yang and J. L. Whitten, Surf. Sci. **255**, 193 (1991).
[19] H. Yang and J. L. Whitten, J. Chem. Phys. **91**, 126 (1989).
[20] H. Yang and J. L. Whitten, J. Chem. Phys. **96**, 5529 (1992).
[21] P. Siegbahn and I. Panas, Surf. Sci. **240**, 37 (1990).
[22] H. Burghgraef, A. P. J. Jansen, and R. A. van Santen, J. Chem. Phys. **98**, 8810 (1993).
[23] H. Burghgraef, A. P. J. Jansen, and R. A. van Santen, Chem. Phys. **177**, 407 (1993).
[24] H. Burghgraef, A. P. J. Jansen, and R. A. van Santen, J. Chem. Phys. **101**, 11012 (1994).
[25] H. Burghgraef, A. P. J. Jansen, and R. A. van Santen, Surf. Sci. **324**, 345 (1995).
[26] A. D. Koster and R. A. van Santen, J. Catal. **127**, 141 (1991).
[27] M. C. Payne, M. P. Teter, D. C. Allen, T. A. Arias, and J. D. Joannopolous, Rev. Mod. Phys. **64**, 1045 (1992), and references therein.
[28] P. Hu, D. A. King, S. Crampin, M. H. Lee, and M. C. Payne, Chem. Phys. Lett. **230**, 501 (1994).
[29] P. Hu, D. A. King, M. H. Lee, and M. C. Payne, Chem. Phys. Lett. **246**, 73 (1995).
[30] J. P. Perdew, J. A. Chevary, S. H. Vosko, K. A. Jackson, D. J. Singh, and C. Fiolhais, Phys. Rev. B **46**, 6671 (1992).
[31] J.-S. Lin, A. Qteish, M. C. Payne, and V. Heine, Phys. Rev. B **47**, 4174 (1993).
[32] L. Kleinman and D. M. Bylander, Phys. Rev. Lett. **48**, 1425 (1982).
[33] H. J. Monkhorst and J. D. Pack, Phys. Rev. B **13**, 5188 (1976).
[34] A. Michaelides and P. Hu, J. Chem. Phys. **112**, 6006 (2000).
[35] A. Alavi, P. Hu, T. Deutsch, P. L. Silvestrelli, and J. Hutter, Phys. Rev. Lett. **80**, 3650 (1998).
[36] C. J. Zhang, P. Hu, and A. Alavi, J. Am. Chem. Soc. **121**, 7931 (1999).
[37] K. Bleakley and P. Hu, J. Am. Chem. Soc. **121**, 7644 (1999).
[38] C. J. Zhang, P. Hu, and M.-H. Lee, Surf. Sci. **432**, 305 (1999).
[39] A. T. Bell and E. Shustorovich, J. Catal. **121**, 1 (1990).
[40] R. A. Periana, D. J. Taube, S. Gamble, H. Taube, T. Satoh, and H. Fujui, Science **280**, 560 (1998).
[41] *Handbook of Chemistry and Physics*, 80th ed., edited by D. R. Lide (Chemical Rubber, London, 1999).